Mini-conference on helicon plasma sources[a)]

E. E. Scime,[1] A. M. Keesee,[1] and R. W. Boswell[2]
[1]*Department of Physics, West Virginia University, Morgantown, West Virginia 26506, USA*
[2]*SP3, Australian National University, Canberra, Australia*

(Received 19 December 2007; accepted 24 January 2008; published online 4 March 2008)

The first two sessions of this mini-conference focused attention on two areas of helicon source research: The conditions for optimal helicon source performance and the origins of energetic electrons and ions in helicon source plasmas. The final mini-conference session reviewed novel applications of helicon sources, such as mixed plasma source systems and toroidal helicon sources. The session format was designed to stimulate debate and discussion, with considerable time available for extended discussion. © *2008 American Institute of Physics*.
[DOI: 10.1063/1.2844795]

I. INTRODUCTION

Although theoretical studies began some years earlier, the modern helicon plasma source has its origin in an experiment conducted by Boswell in 1968 at Flinders University. It was in that experiment that plasma densities greater than 10^{13} cm^{-3} and the first "blue core" argon helicon plasma were obtained. Since that initial helicon source experiment, over 600 journal articles that specifically refer to "helicon plasma" have appeared in the literature (Fig. 1).

The initial helicon and whistler wave theory was developed by Appleton and Hartree, who showed the derivation of a simple relation that described the propagation of electromagnetic waves in a magnetized plasma.[1] In the 1960s, the effect of the Hall term ($\mathbf{j}\times\mathbf{B}$) on the propagation of these waves in terrestrial plasmas was examined by Klosenberg, MacNamara, and Thonemann in the UK[2] and by Legéndy in the United States.[3]

For much of the 1970s and 1980s, helicon sources attracted only modest research attention. However, in the 1990s, researchers looking for plasma sources capable of providing the higher densities needed for a wide range of basic and applied plasma physics experiments rediscovered the helicon source. Research groups employing helicon sources sprang up in Europe, Japan, Korea, and the United States. Helicon sources are now employed for experiments including plasma processing, Alfvén wave propagation, rf current drive, and space propulsion. After peaking in the mid-1990s, the annual "helicon source" publication rate now averages 30–40 journal articles per year. The early history of helicon research, including all the basic theory, was reviewed by Boswell,[4] and helicon research in the subsequent 10 years was reviewed by Chen.[5]

Although efficient plasma production is often the reason that researchers turn to helicon sources, the exact mechanism responsible for coupling the rf power into the plasma is not completely understood. Compared to capacitive and inductive plasma sources operating at similar rf powers, helicon sources clearly yield higher plasma densities, e.g., $n_e \sim 1\times10^{13}$ cm^{-3} for a 1 kW helicon source[6] versus $\sim1\times10^{10}$ cm^{-3} and $\sim1\times10^{11}$ cm^{-3} for capacitive and inductive sources,[7] respectively.

The ionization efficiency of helicon sources was investigated in some depth in the late 1960s[8] and it became clear that neither collisional nor collisionless (Cherenkov damping or Landau damping as it became known) could explain the experimental results. This phenomenon was reinvestigated in the 1980s when Chen suggested that Landau damping in low-power, low-pressure helicons might be responsible for efficient coupling of rf power to the plasma (because wave-particle interactions at the rf wave phase speed could drive electrons at kinetic energies equal to the ionization potential of argon).[9] In the 1990s, both theory[10,11] and experiment[12,13] suggested that damping of the evanescent slow waves on the resonance cone at the plasma edge near the antenna might play a role in plasma production in higher-pressure, higher magnetic field helicon sources operating near the lower-hybrid frequency. Direct measurements of parallel currents consistent with slow waves in the plasma edge[14] did not resolve the controversy as other experimental groups still reported no evidence of slow wave resonance effects.[15] Although the primary focus of most helicon research groups is not investigation of rf coupling in helicon sources, there has been some progress in this area in the 2000s. Therefore, the first session of this mini-conference addressed the issue of "Optimal Helicon Source Performance."

Since a key element of the Landau damping-based rf coupling model (or more correctly, the wave-particle-based coupling model) is the generation of an enhanced electron population moving at the phase velocity of the rf wave, many research groups have looked for energetic electrons in their experiments. Published works include direct[16–18] and indirect[19] measurements of energetic electrons, as well as direct[20] and indirect[21] measurements consistent with very small or nonexistent energetic electron populations. More recently, energetic ions emanating from low-pressure helicon sources with a strong axial density gradient have been reported by multiple helicon source groups.[22–25] Because the existence of energetic particles in helicon sources is relevant to both applications of helicon sources and understanding the fundamental physics of helicon sources, the second session

[a)]Bull. Am. Phys. Soc. **52**, 6 (2007).

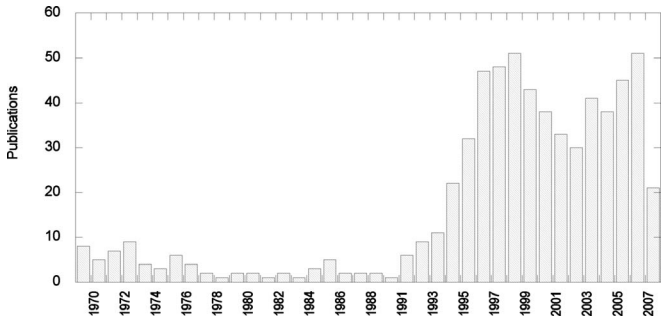

FIG. 1. Number of journal publications per year that refer to "helicon plasma" in the title or abstract.

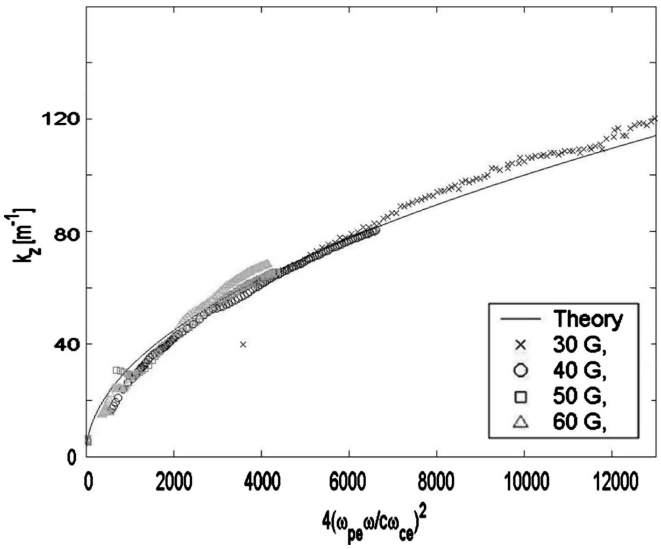

FIG. 2. Variation of $k_{\parallel}$ from B_z measurements for magnetic fields between 30 and 60 G. Adapted from Ref. 41.

of this mini-conference reviewed recent experimental and-computational studies of energetic ion and electron production in helicon sources.

As noted previously, there was a dramatic increase in the use of helicon sources in the 1990s. The unique characteristics of helicon sources operating in various regimes, such as high-efficiency plasma production or the ability to create energetic particles, lend themselves to a wide variety of applications. The third session of this mini-conference highlighted new applications of helicon sources. These new "helicon sources" were designed for magnetohydrodynamic wave studies, toroidal current drive experiments, etc.

In the discussion of the sessions below, only the names of the presenters are given. Coauthors of the talks are listed in volume 51 of the Bulletin of the American Physical Society.

II. OPTIMAL HELICON SOURCE PERFORMANCE

Boswell started off the mini-conference with a review of the classic capacitive to inductive to helicon transition in the low magnetic field WOMBAT (Waves On Magnetized Beams and Turbulence) experiment and a discussion of collisionless wave damping effects. He then presented wave field measurements for a small antenna driven in the whistler frequency regime ($\omega_{ci} < \omega < \omega_{ce}$) and inserted into a background plasma created with a single-loop inductively coupled plasma source. Over a wide range of antenna frequencies, plasma densities, and magnetic fields, he showed that the dispersion of the launched waves obeyed a simple plane-wave whistler dispersion relation (with $k_{\perp} \sim 0$), and not a bounded, cylindrical, whistler "helicon" dispersion relation (see Fig. 2). Boswell argued that this result indicated that for plasma densities greater than 2×10^{11} cm^{-3}, the inertial terms in the full dispersion relation, which give rise to slow-wave solutions (the "Trivelpiece–Gould" mode) and resonance cones, are ignorable because of collisionless Landau damping effects. He also argued that the cylindrical nature of the experiment still forced an $m=1$ periodic solution for the azimuthal wave field and therefore the parallel electric field should peak off-axis at $r \sim a/2$, the same radial location where peak electron heating was also observed. A conference participant suggested that an electron-neutral collision frequency of just four times the rf frequency would be sufficient to reduce the importance of the inertial terms, and therefore his measurements could not uniquely identify the mechanism responsible for reducing the contributions of the inertial terms to the whistler dispersion relation for his plasma parameters.

Next, Goulding presented hydrogen plasma density measurements obtained during low-power (1.2 kW) and high-power (5 kW) operation of the mini-RFTF (Mini-Radio Frequency Test Facility) helicon experiment at Oak Ridge National Laboratory. At low power, optimal performance (highest density, $n_e \sim 5 \times 10^{12}$ cm^{-3}) was obtained [Fig. 3(a)] when the rf frequency (21 MHz) equaled the lower hybrid frequency ($\omega_{LH} \approx \sqrt{\omega_{ce}\omega_{ci}}$ for 100 G $< B <$ 400 G). However, at high power, similar performance was obtained for rf frequencies above and below the lower hybrid frequency [Fig. 3(b)]. Goulding then presented measurements of the perpendicular wave number obtained from the axial helicon wave field in high-power plasmas which, for magnetic fields such that the $B/B_{LH} < 1$ (where B_{LH} is the magnetic field at which the lower hybrid frequency equals the rf driving frequency), were consistent with predictions for the second radial eigenmode of the helicon wave. For $B/B_{LH} > 1$, the measurements were consistent with excitation of the first radial eigenmode. Simulation runs using the two-dimensional (2D) EMIR3 code, which combines power and particle balances as well as collisional effects with a cold plasma dielectric, were able to reproduce the observed radial mode structure, peaked radial density profile, and axial peaking of the plasma density downstream of the antenna—purely from collisional damping of the helicon wave.[26] Questions from the audience focused on the radial transport levels required to explain the mini-RFTF density values and radial profiles. Goulding suggested that the mini-RFTF measurements were consistent with classical levels of radial transport, i.e., sub-Bohm radial diffusion.

Balkey then presented electron density, electron temperature, and ion temperature measurements from the

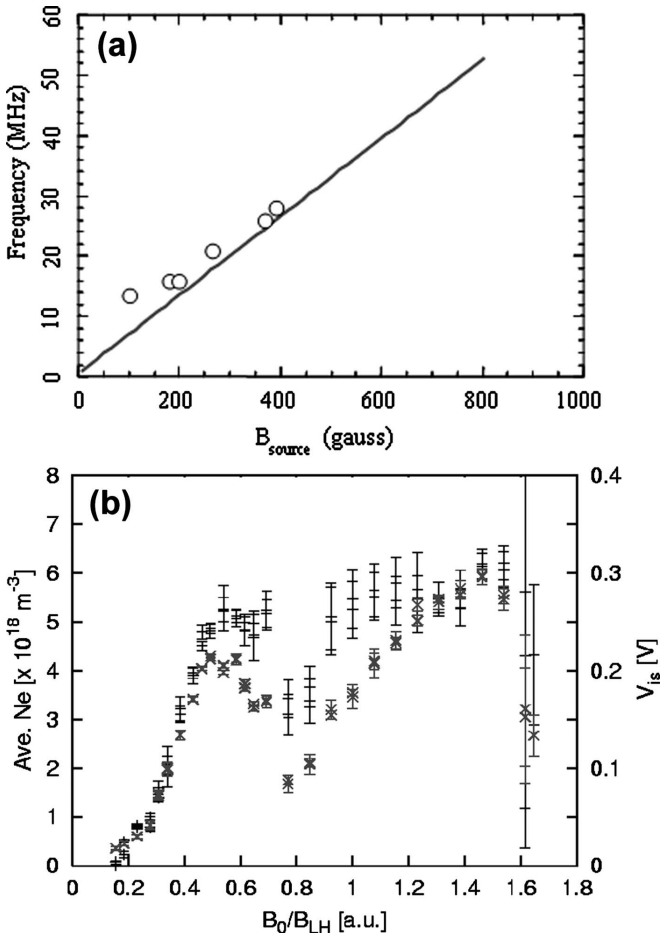

FIG. 3. (a) Optimal operating frequency, for highest density plasmas (○) and lower hybrid frequency vs source magnetic field strength. (b) Hydrogen plasma density measured by interferometry (vertical dashes) and a Langmuir probe (×) vs magnetic field strength normalized to the magnetic field strength required to match the lower hybrid frequency to the rf frequency. Adapted from Refs. 8 and 21.

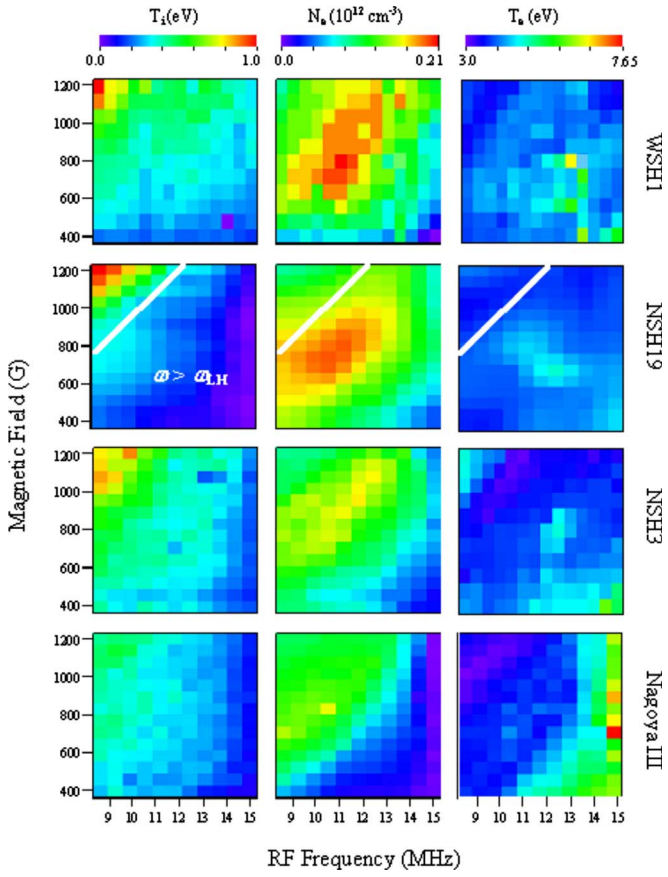

FIG. 4. (Color online) Perpendicular ion temperature, downstream electron density, and downstream electron temperature vs magnetic field strength and rf frequency for a wide strap 19 cm long antenna (first row), a narrow strap 19 cm antenna (second row), narrow strap 30 cm long antenna (third row), and a Nagoya III antenna (fourth row). All plots of each parameter are on the same color bar scale that is shown at the top of each column. Adapted from Ref. 42.

HELIX (Hot hELIcon eXperiment) helicon source operating at an rf power of 0.75 kW, over a range of rf frequencies and magnetic field strengths, and for four different antenna configurations (Fig 4). Peak electron densities were obtained when $\omega=\sqrt{\omega_{ce}\omega_{ci}}$ on the source axis. However, peak ion temperatures were obtained for $\omega=\omega_{\mathrm{LH}}$ at the plasma edge, where $1/\omega_{\mathrm{LH}}^2(r)\cong 1/[\omega_{pi}^2(r)+\omega_{ci}^2]+1/(\omega_{ce}\omega_{ci})$. Later measurements in a modified version of the same source confirmed peak ion temperatures were obtained when the rf frequency equaled the lower hybrid frequency in the plasma edge and that the perpendicular ion temperature was peaked at the plasma edge while the parallel ion temperature was peaked on axis for the same conditions.[27] Balkey argued that these measurements demonstrated a clear lower hybrid resonance effect, and therefore slow waves (TG modes) are involved in the coupling of the rf power into helicon sources operating at powers on the order of 1 kW, pressures of a few mTorr, and magnetic field strengths such that a lower hybrid resonance is achieved at a specific radial location in the plasma column. Mini-conference participants pointed out that if the input power was held fixed in all the cases shown, the final disposition of the "missing" power in the low performance cases was not identified. Others in the audience also argued that at higher rf powers, the lower hybrid effects would disappear and the coupling would be dominated by coupling to specific radial eigenmodes.

Chen then presented a discussion of radially localized helicon (RLH) waves,[28] where the radial localization arises from the steep radial density profile and the large length-to-diameter ratio of helicon sources. The fundamental difference between "classic" whistler waves and RLH waves is that for the case of RLH waves, $\omega\approx k_{\parallel}^2\omega_{ce}c^2/\omega_{pe}^2$, whereas for whistler waves, $\omega\approx kk_{\parallel}\omega_{ce}c^2/\omega_{pe}^2$. In a series of experiments using a background helicon plasma and an additional, low-power, perturbing antenna at the University of Texas at Austin, Panevsky and Bengtson demonstrated the existence of a RLH wave resonance at the predicted frequency (predicted by theory and by a 2D electromagnetic wave solving code) given their source geometry.[29] The observed wave damping rate (width of the resonance feature) was consistent with purely collisional wave damping. The 2D code also predicted off-axis peak electron heating and power absorption by TG modes of only 10% of the total rf power absorption. Conference participants noted that the $\omega\propto k_{\parallel}^2$ scaling of

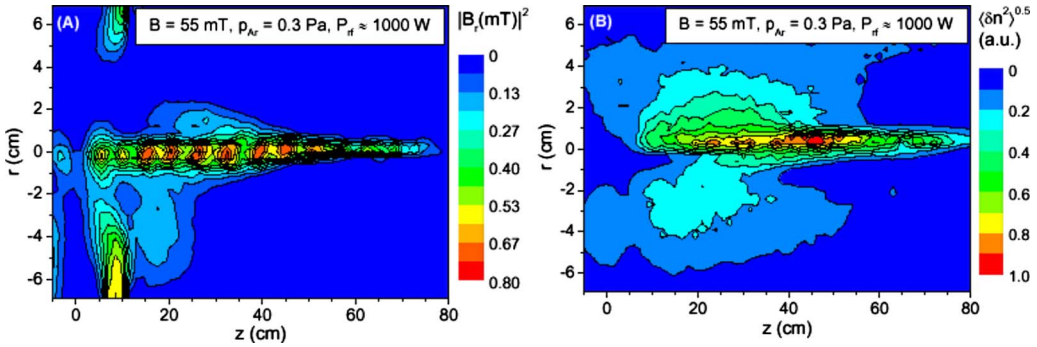

FIG. 5. (Color online) Time-resolved measurements of (a) rf wave energy and (b) plasma density vs radial and axial location. The wave energy propagates downstream toward a well-defined, downstream peak in the electron density. Adapted from Ref. 43.

RLH waves is consistent with the independent perturbing wave experiments in WOMBAT reported earlier in the mini-conference by Boswell (Fig. 2). Concerns were raised that the model results were restricted to density profiles with discontinuous density steps. However, Chen responded that similar results could be obtained with smooth density profiles. Another concern raised by participants was that the predicted resonances depended strongly on the source length, and that for systems over a few meters long, or without fixed axial boundaries, the RLH resonance decreases to frequencies less than 1 MHz.

Kramer wrapped up the first oral session of the mini-conference with a presentation of high- (1.5 kW) and low- (0.1 kW) power pulsed helicon experiments in the HE-L source. By 1 ms into the high-power discharges (B =540 G), a well-defined peak in the plasma density appeared ~20 cm downstream of the $m=+1$ helical antenna. Time-resolved measurements of the radial component of the wave magnetic field indicated propagation of waves with perpendicular wave numbers of approximately $k_\perp \sim 100$ m^{-1} from the plasma edge toward the axis of the source. The density profile in the high-power discharges was sharply peaked off-axis, whereas the density profile of the low-power discharges was peaked on the source axis. Kramer argued that, for the low-power discharges, measurements of the axial damping of the B_z wave field and comparisons with an EMHD (electron fluid magnetohydrodynamic) model were inconsistent with linear damping of the helicon waves, i.e., simple collision damping was insufficient to explain the observations. Kramer then presented wave field energy and electrostatic fluctuation measurements in high-power discharges, which showed a spatial correlation between maxima in the rf wave energy and strong electrostatic fluctuations (Fig. 5). He then suggested that the enhanced fluctuations were evidence of parametrically driven instabilities, which in turn could explain the enhanced wave damping rates downstream of the antenna. Questions from the participants concerned the fraction of rf power absorbed downstream of the antenna. Based on the measurements, Kramer estimated that 80% of the rf power was absorbed directly under the antenna and 20% in the downstream volume—and even with only 20% of the total rf power available, the plasma density was still peaked downstream of the antenna.

III. ENERGETIC IONS AND ELECTRONS IN HELICONS

The second oral session began with Sefkow's presentation of particle-in-cell (PIC) modeling results motivated by experiments in the MNX (Magnetic Nozzle eXperiment) helicon source. In the cylindrical PIC model, a mechanical aperture is located upstream (1.5 cm) of a maximum in magnetic field created by a magnetic nozzle coil; the magnetic field converges and increases into the downstream expansion region (ER). The PIC code included Coulomb collisions, charge-exchange collisions, and electron-impact ionization of neutral argon. For an imposed neutral pressure gradient of 0.75 mTorr upstream to 0.25 mTorr downstream or an imposed uniform background neutral pressure, the PIC code predicts formation of a 0.3–0.4 cm thick sheath (~200–300 λ_D) near the mechanical aperture. Both initial ions and neutral atoms that become ionized in the simulation are accelerated from the source region to the expansion region by the sheath. As shown in Fig. 6, the ions are accelerated to energies ~3 T_e across the sheath at the aperture and then undergo further acceleration to ~6 T_e over another 2 cm in the ER—consistent with recent measurements of small apertures producing ion beams.[30] Near the axis and within the aperture

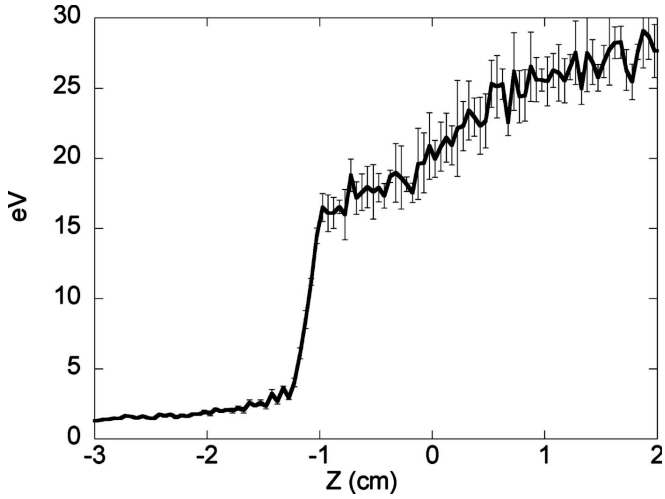

FIG. 6. Ion energy as a function of position in the PIC simulation. Adapted from Ref. 44.

radius, the PIC model also predicts a two-component electron velocity distribution function (also consistent with recent measurements[31]) and excitation of ion acoustic waves in the acceleration region. During the discussion, Sefkow noted that to handle spatial scales smaller than λ_D in the simulation, the PIC code employed a completely energy-conserving algorithm. However, electron energy losses through excitation collisions were not included. Conference participants questioned the self-consistency of the model given how the initial plasma was created. Sefkow argued that although the PIC model did not include the rf helicon waves, the injection region to the left of the simulation (not shown in Fig. 6) was self-consistent in terms of plasma density and plasma potential.

Speaking on behalf of C. Charles, Boswell presented recent measurements from the low magnetic field strength Chi–Kung source. In 0.5 kW, 0.07 mTorr xenon plasmas, a highly collimated 50 eV ion beam (divergence less than 6°) was observed. Formation of the beam could be triggered and then controlled by increasing the magnetic field strength of the downstream electromagnet in the two electromagnet, Helmholtz coil, configuration of Chi–Kung.[32] Boswell noted that these experiments demonstrated direct control of the specific impulse if this type of source were to be employed as a plasma thruster. During discussion of the physics responsible for the magnetic field strength induced transition, Boswell noted that, coincident with the appearance of the ion beam, the upstream to downstream density ratio increased dramatically and the radial potential profile in the upstream region became nearly flat—suggesting a sharp reduction in radial transport in the upstream region.

Moving on to the possible existence of energetic electrons in helicon sources, Keesee presented emission spectroscopy and laser-induced-fluorescence (LIF) measurements of the radial profiles of Ar I state populations in the HELIX source.[21] Keesee's experiments were designed to determine, through a combination of spectroscopic measurements and collisional-radiative (CR) modeling, the neutral density radial profile in helicon sources. For a 0.3 kW, 750 G, 6.0 mTorr fill pressure argon helicon plasma, Keesee reported that a 65% on-axis neutral depletion best fit both the Abel-inverted emission spectroscopy and LIF measurements. The best-fit depletion region extended over the inner 60% of the source. Addition of an energetic electron population (20 eV directed kinetic energy with a 0.01 eV beam temperature) with a beam density of just 0.1% of the bulk electron population resulted in Ar I state population profiles that could not be simultaneously reconciled with the LIF and spectroscopic measured profiles. Keesee therefore argued that, at least for helicon sources operating at moderate neutral pressures, there was no spectroscopic evidence of energetic electrons. In response to a question, Keesee explained that other possible neutral ground-state profiles with an electron beam were considered, but the neutral density profile presented remained the best fit to the LIF and line emission measurements. In response to another question, Keesee noted that the Ar I collisional radiative model was limited to neutral pressures greater than a few mTorr. For lower pressures, a coronal model would be more appropriate.

Scharer then presented high-time resolution measurements of Ar II 443 nm emission that were synchronized with the driving rf antenna in WOMBAT and in the UW-Madison helicon facility. The upper state for the 443 nm Ar II emission is 35 eV above the ion ground state (which itself requires 15.6 eV for creation from neutral argon). In the high-power (2.3 kW), low magnetic field (100 G), and 3 mTorr neutral pressure WOMBAT experiments, Scharer observed 25% modulation of the 443 nm emission and a phase difference in the peak of emission that increased with increasing distance from the rf antenna. Interpreting these results as evidence of energetic electrons being driven by the rf wave, the energies of the moving electrons were in the range 30–52 eV, consistent with the phase velocity of the rf wave as determined from magnetic field fluctuation measurements.[33] Similar results were obtained for 443 nm emission in moderate power (0.8 kW) inductive mode experiments at UW–Madison. However, when the rf power was increased and the blue-core helicon mode obtained, there was no evidence of any rf wave synchronous modulation of the 443 nm emission. Scharer then presented measurements of plasma density versus rf power, neutral pressure, and magnetic field strength that he argued were consistent with neutral depletion limiting the amount of plasma density that could be created in the source. Mini-conference participants questioned why, if energetic electrons (presumably driven by wave-particle interactions) were responsible for plasma production in helicon sources, there was no correlation in 443 nm emission once the source transitioned to the high-density, blue-core, helicon mode. Scharer argued that the blue-core helicon plasmas were more collisional and the increased collisionality thermalized the Landau-damping driven electrons before they could excite the necessary Ar II state.

Returning to simulation results, Meige presented recent results from PIC modeling of high-power (2 kW), pulsed, unmagnetized, Ar/SF_6 highly electronegative plasmas in which double layers propagating toward the source region have been observed.[34] Meige employed a hybrid model (PIC ions and Boltzmann electrons) to calculate the spatially resolved plasma potential and a Monte Carlo algorithm (PIC electrons) to determine the electron temperature and the attachment, recombination, ionization, and electron-neutral collision rates. In both theory and experiment, multiple double-layer-like structures were observed within a larger propagating structure (Fig. 7). Meige argued that the small size of the source chamber, compared to the electron mean free path, and rf heating of the electrons in the source lead to enhanced losses of electrons in the source region and increased source electron temperature. These effects result in positive ions being created in the source and negative ions in the downstream region. If the source is long enough, as the different charge ions drift toward each other they reach the Bohm speed and quasineutrality is violated, i.e., a sheath forms. Meige suggested that the propagating nature of the sheath might result from a modest imbalance in the internal forces in the double-layer. Conference participants were most interested in the prediction of a threshold chamber length for double-layer formation in these highly electrone-

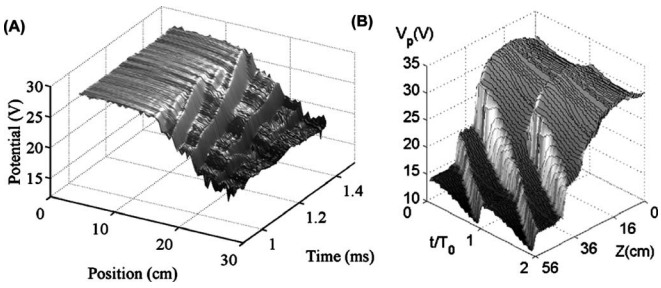

FIG. 7. Simulation of propagating double layers in an electronegative plasma. Adapted from Ref. 34.

gative plasmas, a prediction Meige noted was consistent with recent experimental observations.[35]

Speaking on behalf of E. Sciamma, Bengtson presented results from a series of experiments designed to determine absolute values of electron temperature and neutral density from spectroscopic measurements of Ar I and Ar II line emission along with Langmuir probe measurements of the plasma density. Bengtson showed that for helicon plasmas of density $\sim 8\times 10^{12}$ cm^{-3}, absolutely calibrated measurements of Ar II lines from 425 to 525 nm combined with the ADAS Ar II collisional-radiative model[36] yielded electron temperatures of 3.7 eV, consistent with the Langmuir probe electron temperature results. For that electron temperature, the Ar I collisional-radiative model[21] predicted a total neutral density of $\sim 4\times 10^{13}$ cm^{-3}, consistent with the measured edge neutral pressure of 1 mTorr ($\sim 3\times 10^{13}$ cm^{-3}) and corresponding to an ionization fraction of 13%. In response to questions, Bengtson reported that no Ar III lines were observed in their experiments.

IV. WHAT'S NEXT FOR HELICON SOURCES?

Watts started off the final session of the mini-conference with a description of the combined helicon–solid oxide cathode plasma source (HELCAT) at the University of New Mexico. In a previous incarnation, Watts' source had included seven independent helicon sources in a close-packed hexagonal array with a goal of creating a large volume, uniform high-density plasma.[37] However, reducing the background magnetic field to levels at which the gyroradius of the argon ions equaled the source-to-source spacing (so as to eliminate the sharp field-aligned density peaks that arise from seven blue-core plasmas at different radial and azimuthal locations) also resulted in unstable plasmas with maximum argon plasma densities of only $\sim 10^{12}$ cm^{-3}. For the combined cathode-helicon system, Watts reported helium plasma densities of $\sim 10^{12}$ cm^{-3} for the 250 ms long, 0.8 kW, single helicon source pulse for a fill pressure of 0.5 mTorr. Watts noted that the 1000 °C cathode heater appears to eliminate the need for a high-power startup pulse to initiate breakdown in helium plasmas. A 10 ms cathode pulse of 500 A is triggered 50 ms into the discharge and the plasma density drops slightly while the electron temperature rises slightly and the electron temperature radial profile flattens. Complete recovery to the precathode pulse conditions takes approximately 40 ms. In response to questions, Watts noted that a variety of magnetic field configurations were tried to "mix" the seven independent helicon source "blue-cores," e.g., magnetic nozzles and mirror fields, but none were successful at producing a stable and uniform large-area plasma.

Next, Masters presented results from a short length, 0.4 kW source in which the Nagoya III antenna was inserted into the plasma. In a background pressure of 3 mTorr, plasma densities of $\sim 1\times 10^{13}$ cm^{-3} were obtained only when there was no background axial magnetic field. In fact, magnetic field strengths of a few hundred Gauss appeared to extinguish the plasma. Masters argued that measurements of the cylindrical components of the wave magnetic fields suggest a combination of $m=+1$ and $m=0$ helicon modes were being excited. In response to questions, Masters noted that erosion of the fiberglass tape and spray-on boron-nitride coating on the internal antenna limited steady-state operation to moderate powers (approximately a few hundred Watts). Once the insulation failed, the plasma source either failed to ignite or operated in an unstable manner.

Next in the session was a review of toroidal helicon experiments at the Institute for Plasma Research in Gandhinagar, India. Kumar-Paul began by outlining the modifications to the cylindrical helicon wave fields that arise from a toroidal geometry.[38] He then described initial experiments in a 30-cm major radius, 10.5-cm minor radius torus with a maximum magnetic field strength of 1 kG, rf power of 2 kW provided in 50 ms pulses (at 7–9 MHz), argon fill pressures of 2–5 mTorr, and an internal helical antenna. Plasma densities of $\sim 1\times 10^{12}$ cm^{-3} and electron temperatures of 10 eV were obtained. More significantly, for magnetic field strengths such that the rf frequency approximated the lower hybrid frequency, nearly 1 kA of toroidal current was driven.[39] Kumar-Paul then described more recent experiments performed at higher rf frequencies (32 MHz) that were designed to investigate the possibility of nonresonant current drive through ponderomotive effects and the net helicity of toroidal helicon waves. Nearly 100 A of toroidal current was driven nonresonantly in those experiments (Fig. 8).[40] Based on the rapid disappearance of the current drive when the plasma dropped out of the helicon mode, Kumar-Paul argued that the helicon mode was essential for the nonresonant current drive process. In response to questions, Kumar-Paul noted that the plasmas never reached a "blue-core" helicon mode and that neither the radial transport nor the particle confinement in the toroidal helicon plasmas had yet been determined.

Batischev then presented recent results from the mini-Helicon Thruster Experiment (mHTX), a compact (2 cm diameter), high-power density (1 kW), prototype thruster. Batischev reported successful operation in multiple gases, e.g., Ar, Ne, Xe, N_2, and air, and observations of ion flow downstream of the Helmholtz coil set used to create the magnetic field in the source. Mach probe and high-resolution spectroscopic measurements indicated ion flows of up to 21 km/s in the plasma plume at the end of the source. In response to questions, Batischev noted that the exit ion flow

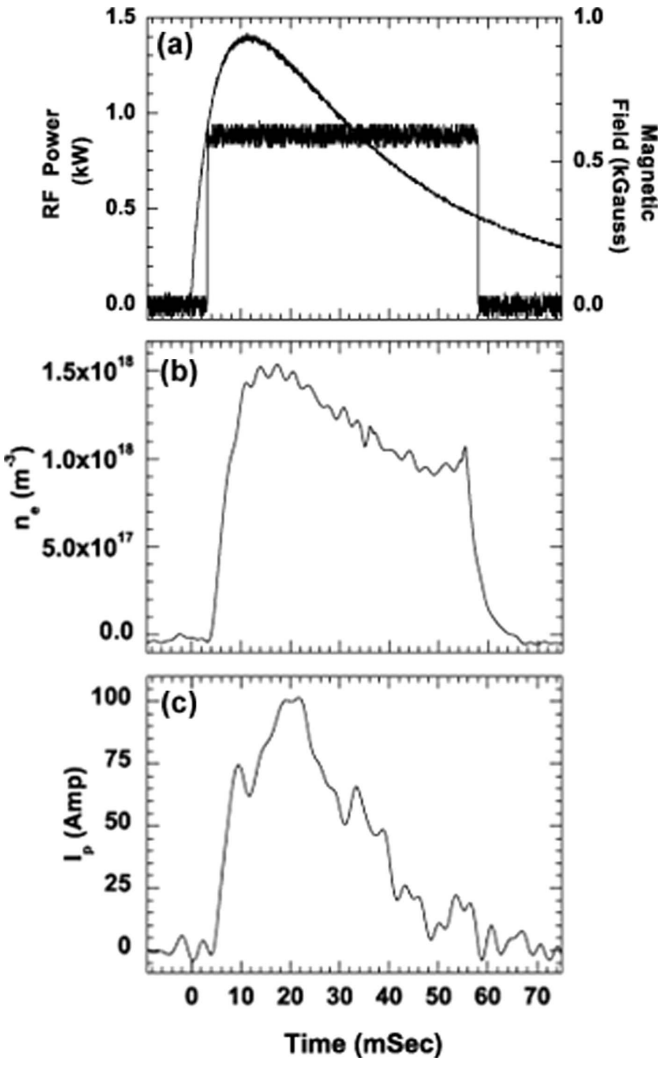

FIG. 8. (a) rf power and magnetic field current waveforms, (b) plasma density, and (c) nonresonant driven toroidal current vs time for the toroidal helicon source. Adapted from Ref. 40.

speed increased with decreasing input neutral gas flow rates.

Berisford wrapped up the "What's Next for Helicon Sources" session with a presentation of total power balance measurements in a 1.0 kW, 600 G, argon helicon source built around a short Pyrex tube coupled to a roughly 1 m stainless-steel expansion chamber. With an absolutely calibrated IR camera, internal plasma and thermocouple probes, and an endplate bolometer, Berisford was able to measure the final disposition of the input rf power in terms of heat deposited throughout the plasma source system. He reported that 17% of the input power appeared as heat in the glass tube (15% in the tube under the antenna and 2% upstream of the antenna), 74% was lost to the walls of the expansion chamber, and 1% was deposited on the endplate of the expansion chamber. IR camera measurements of the interior of the matching network identified another 5% of the input power deposited as heat in the matching network. The sum of all the measured losses equaled 97% of the input power. When the magnetic field direction was reversed, the energy deposited upstream of the antenna jumped to 25% of the input power, thereby confirming that helicon sources preferentially couple rf power downstream of the antenna in the $m=+1$ configuration. Conference participants noted that the missing 3% of power might be lost through pumping of exhaust gasses and that these measurements highlighted the effectiveness of helicon sources in coupling rf power into the exhaust plume in thruster-like configurations.

V. PERSPECTIVES OF THE ORGANIZERS

A. Boswell

The as yet unexplained dispersion of helicons/whistlers in cylinders seems to be heading for a denouement with remarkable similarity between the results of the theory group at Austin and the experimental results at the ANU. The former propose a "radial resonance" induced by strong radial gradients that leads to the elimination of $k_\perp$ from the dispersion, whereas the latter propose that the cusps and resonance cone effects in the surfaces of constant phase are removed leaving the pure electromagnetic (Hall term) of the dispersion. Presumably further work will ensue from this.

The problem of power coupling to the "blue core" observed in argon plasmas is still unexplained with columns of over 100 cm long showing powerful ArII emissions along the axis that can only come from locally accelerated electrons. Electromagnetic energy must propagate down the center of the plasma column and electrons must be accelerated in the parallel electric fields of these waves as this is where the excited ion emission is seen. Hence waves must be accelerating the electrons in some manner that is not yet understood.

B. Scime

Listening to the speakers in the first session, I was struck by the key role played by a steep density profile in all of the theoretical, numerical, and experimental discussions. In Chen's work, the strong radial variation in density led to a plane-wave-like dispersion relation that was startlingly similar in its $\omega \propto k_\parallel^2$ scaling to the experimental whistler wave measurements of Boswell. In Balkey's presentation, the steep density profile resulted in ion inertia contributions to the lower hybrid frequency and shifting of the lower hybrid resonance toward the low density plasma edge, where strong ion heating appeared for rf frequencies less than the lower hybrid frequency. In Balkey's and Goulding's works, lower hybrid resonance effects (improved performance) appeared at low rf powers, but vanished at high powers, i.e., when the plasma density was large throughout the device and ion inertial effects in the lower hybrid resonance were ignorable. In Chen's model, resonant behavior was strongly tied to the axial boundary conditions but modest power absorption also occurred at the lower hybrid resonance in the plasma edge and the absorption moved toward the system axis further downstream. Whether or not enhanced performance appears at rf frequencies around the lower hybrid frequency seems to

depend strongly on whether or not the lower hybrid resonance is localized to the plasma edge—in the very region where the slow waves are most strongly damped. Even Kramer's observations of parametrically driven fluctuations in moderate power (<2 kW) helicon plasmas, and enhanced rf damping, are tightly coupled to excitation of slow, TG, modes.

The self-consistent model that emerges is that for a steep density profile in an axially bounded system, eigenmode resonances can be an important factor in coupling rf power into the plasma through the collisional damping of the helicon wave. However, without axial boundaries, the eigenmode resonances drop to low frequencies and a steep density profile still leads to whistler wave dispersion in the plasma core that is more plane-wave-like than a classic helicon wave. When low densities in the plasma edge shift the lower hybrid resonance out to the plasma edge, resonant damping of the slow wave leads to ion heating, increased plasma density, and parametrically driven fluctuations. Raising the rf power above a few kW, thereby raising the overall plasma density, eliminates any spatial localization of the lower hybrid resonance, and then for an axially bounded system, collisional damping of the eigenmode resonance for helicon waves become important again. Such a physical picture is consistent with the measurements and models of the wide variety of helicon sources existing today.

That some research groups have found evidence of energetic electrons in helicon sources, particularly in low-density, non-blue-core mode helicon sources, seems clear. However, in high-density helicon plasmas, both the direct and indirect measurements suggest that any energetic electron population, if present, does not play a significant role in the ionization of neutrals or the excitation of ions. If the question is, "Do wave-particle interactions create a population of energetic electrons that play a primary role in plasma creation in high-density helicon sources?" The answer is "no."

As described in this mini-conference, all sorts of source configurations seem to be able to produce ion beams, e.g., electronegative plasmas, simple expanding helicon plasmas, and helicon sources restricted by a small aperture. Common to all these systems is a strong plasma density gradient. Independent of magnetic field gradients and background neutral pressure gradients, it appears that whatever structure forms to create the sharp potential drop responsible for the ion acceleration does so at the same time a sharp upstream-downstream gradient in the plasma density forms. A growing body of evidence suggests that the plasma density gradient is related to unequal plasma loss rates in the upstream and downstream regions when the mean free paths of the plasma constituents become comparable to the dimensions of the plasma source.

Finally, the variations on the helicon source theme continue to grow: Internal antennae, exotic mixed gasses, thrusters, and toroidal helicons—all evidence of a vibrant community of helicon source users.

ACKNOWLEDGMENTS

The mini-conference organizers gratefully acknowledge the many contributions to helicon source research by the participants in the mini-conference, by the many colleagues whose work is referenced in this manuscript, and the innumerable colleagues whose work was not cited in this manuscript due to space limitations. E.E.S. and A.M.K. acknowledge support for this work from NSF award No. PHY-0611571.

[1] E. V. Appleton, J. Inst. Electr. Eng. **71**, 642 (1932).
[2] J. P. Klosenberg, B. McNamara, and P. C. Thonemann, J. Fluid Mech. **21**, 545 (1965).
[3] C. R. Legéndy, Phys. Rev. **135**, 1713 (1965).
[4] R. W. Boswell and F. F. Chen, IEEE Trans. Plasma Sci. **25**, 1229 (1997).
[5] F. F. Chen and R. W. Boswell, IEEE Trans. Power Appar. Syst. **25** 1245 (1997).
[6] R. W. Boswell, Plasma Phys. Controlled Fusion **26**, 1147 (1984).
[7] M. A. Lieberman and A. J. Lichtenberg, *Principles of Plasma Discharges and Material Processing* (John Wiley & Sons, New York, 2005), p. 14.
[8] R. W. Boswell, "A study of waves in gaseous plasmas," Ph.D. thesis, Flinders University, Adelaide, Australia (1974). Available at http://www.heliconrefs.com.
[9] F. F. Chen, Plasma Phys. Controlled Fusion **33**, 339 (1991).
[10] K. P. Shamrai and V. B. Taranov, Phys. Lett. A **204**, 139 (1995).
[11] S. Cho, Phys. Plasmas **7**, 417 (2000).
[12] J. L. Kline, E. Scime, R. Boivin, A. M. Keesee, X. Sun, and V. Mikhailenko, Phys. Rev. Lett. **88**, 195002 (2002).
[13] J. P. Squire, F. R. Chang-Diaz, T. W. Glover, V. T. Jacobson, G. E. McCaskill, D. S. Winter, F. W. Baity, M. D. Carter, and R. H. Goulding, Thin Solid Films **506–507**, 597 (2006).
[14] D. D. Blackwell, T. G. Madziwa, D. Arnush, and F. F. Chen, Phys. Rev. Lett. **88**, 145002 (2002).
[15] M. Light, F. F. Chen, and P. L. Colestock, Plasma Sources Sci. Technol. **11**, 273 (2002).
[16] A. R. Ellingboe, R. W. Boswell, J. P. Booth, and N. Sadeghi, Phys. Plasmas **2**, 1807 (1995).
[17] R. T. S. Chen and N. Hershkowitz, Phys. Rev. Lett. **80**, 4677 (1998).
[18] A. W. Molvik, A. R. Ellingboe, and T. D. Rognlien, Phys. Rev. Lett. **79**, 233 (1997).
[19] J. Scharer, A. Degeling, G. Borg, and R. Boswell, Phys. Plasmas **9**, 3734 (2002).
[20] D. D. Blackwell and F. Chen, Plasma Sources Sci. Technol. **10**, 226 (2001).
[21] A. M. Keesee and E. E. Scime, Plasma Sources Sci. Technol. **16**, 742 (2007).
[22] C. Charles and R. W. Boswell, Appl. Phys. Lett. **82**, 1356 (2003).
[23] S. A. Cohen, N. S. Siefert, S. Stange, R. F. Boivin, E. E. Scime, and F. M. Levinton, Phys. Plasmas **7**, 2593 (2003).
[24] X. Sun, A. M. Keesee, C. Biloiu, E. E. Scime, A. Meige, C. Charles, and R. W. Boswell, Phys. Rev. Lett. **95**, 025004 (2005).
[25] N. Plihon, C. S. Corr, and P. Chabert, Appl. Phys. Lett. **86**, 091501 (2005).
[26] M. D. Carter, F. W. Baity, G. C. Barber, R. H. Goulding, Y. Mori, D. O. Sparks, K. F. White, E. F. Jaeger, F. R. Chang-Diaz, and J. P. Squire, Phys. Plasmas **9**, 5097 (2002).
[27] J. L. Kline, E. Scime, R. Boivin, A. M. Keesee, and X. Sun, Plasma Sources Sci. Technol. **11**, 413 (2002).
[28] B. N. Breizman and A. V. Arefiev, Phys. Rev. Lett. **84**, 3863 (1999).
[29] M. Panevsky and R. Bengtson, Phys. Plasmas **11**, 4196 (2004).
[30] X. S. Sun, S. Cohen, and E. E. Scime, Phys. Plasmas **12**, 103509 (2005).
[31] S. Cohen, X. Sun, and E. E. Scime, IEEE Trans. Plasma Sci. **34**, 792 (2006).
[32] C. Charles and R. Boswell, Appl. Phys. Lett. **91**, 201505 (2007).
[33] J. Scharer, A. Degeling, G. Borg, and R. Boswell, Phys. Plasmas **9**, 3734 (2003).
[34] A. Meige, N. Plihon, G. J. M. Hagelaar, J.-P. Boeuf, P. Chabert, and R. W. Boswell, Phys. Plasmas **14**, 053508 (2007).
[35] N. Plihon, C. S. Corr, P. Chabert, and J.-L. Raimbault, J. Appl. Phys. **98**, 023306 (2005).
[36] For details of the ADAS model, see http://adas.phys.strath.ac.uk/newline.

[37]C. Watts, Rev. Sci. Instrum. **75**, 1975 (2004).
[38]S. K. P. Tripathi and D. Bora, Phys. Plasmas **8**, 697 (2001).
[39]S. K. P. Tripathi and D. Bora, Nucl. Fusion **42**, L15 (2002).
[40]M. Kr. Paul and D. Bora, Phys. Plasmas **14**, 082507 (2007).
[41]A. W. Degeling, G. G. Borg, and R. W. Boswell, Phys. Plasmas **11**, 2144 (2004).
[42]M. Balkey, R. Boivin, P. A. Keiter, J. L. Kline, and E. Scime, Plasma Sources Sci. Technol. **10**, 284 (2001).
[43]M. Kramer, Bull. Am. Phys. Soc. **52**, GM5.00005 (2007).
[44]S. Cohen and A. Sefkow, Bull. Am. Phys. Soc. **52**, JM5.00001 (2007).